Analysis of Joint Multiband Sensing-Time M-QAM Signal Detection in Cognitive Radios

Sana Tariq, Abdul Ghafoor, and Salma Zainab Farooq

We analyze a wideband spectrum in a cognitive radio (CR) network by employing the optimal adaptive multiband sensing-time joint detection framework. This framework detects a wideband M-ary quadrature amplitude modulation (M-QAM) primary signal over multiple nonoverlapping narrowband Gaussian channels, using the energy detection technique so as to maximize the throughput in CR networks while limiting interference with the primary network. The signal detection problem is formulated as an optimization problem to maximize the aggregate achievable secondary throughput capacity by jointly optimizing the sensing duration and individual detection thresholds under the overall interference imposed on the primary network. It is shown that the detection problems can be solved as convex optimization problems if certain practical constraints are applied. Simulation results show that the framework under consideration achieves much better performance for M-QAM than for binary phase-shift keying or any real modulation scheme.

Keywords: Cognitive radio, wideband Gaussian primary signal, convex optimization, M-QAM.

Manuscript received Apr. 23, 2012; revised Sept. 12, 2012; accepted Sept. 21, 2012.

Sana Tariq (phone: +92 51 561 5233345, sanatariq@mcs.edu.pk) and Abdul Ghafoor (corresponding author, abdulghafoor-mcs@nust.edu.pk) are with the Department of Electrical Engineering, Military College of Signals, National University of Sciences and Technology, Islamabad, Pakistan.

Salma Zainab Farooq (zaineb.farooq@ist.edu.pk) was with the Department of Electrical Engineering, Military College of Signals, National University of Sciences and Technology, Islamabad, Pakistan, and now is with the Department of Electrical Engineering, Institute of Space Technology Islamabad, Pakistan.

http://dx.doi.org/10.4218/etrij.12.1812.0043

I. Introduction

To combat the spectrum shortage faced due to the fixed spectrum allocation policy by agencies all over the world, cognitive radio (CR) has been proposed as a potential solution. A CR supports the efficient use of the spectrum by finding the existence of spectrum holes. These spectrum holes play a key role in optimizing the given bandwidth by allowing secondary users (SUs) to transmit data when the primary user (PU) is inactive [1]. To enable dynamic spectrum access, the SU must monitor the local spectrum periodically and detect the spectrum holes through spectrum sensing [2], [3].

For maximum spectrum utilization, a wideband spectrum should be considered for secondary transmission opportunities. Generally, this wideband spectrum is divided into multiple nonoverlapping narrowband subchannels. These subbands are then down-converted and digitized and can be analyzed in parallel [4]-[10] or sequentially [11]-[15]. Sequentially sensing the wideband spectrum is time-consuming compared to the parallel sensing approach, as the latter permits efficient management of a wideband spectrum, due to simultaneous detection of the primary signal across multiple frequency bands at the cost of detection hardware [16].

In the multiband sensing-time joint detection (MSJD) framework [7]-[9], the channel sensing problem is devised by dividing the wideband channel into nonintersecting contiguous subbands. The SU senses these subchannels periodically for sensing opportunities or vacating the channels when the PU reappears so as to impose minimum interference with the PU. The spectrum sensing problem is formulated as an optimization one, in which the objective is to maximize the secondary throughput. This optimization problem is further simplified as convex by imposing some practical conditions.

Hoseini and Beaulieu [7], [8] determined the problem to be convex when the primary signal is complex phase-shift keyed (PSK) and the channel is circularly symmetric complex Gaussian (CSCG). In previous work [9], an analysis of the MSJD framework for the primary signal and channel that are CSCG was done, and the range for which the MSJD framework is convex was presented.

In [17], Latif concluded that M-ary quadrature amplitude modulation (M-QAM) modulated signals can be easily utilized in high data rate applications providing more power efficiency than a complex PSK modulated signal can provide, while providing the same bandwidth efficiency as compared to a complex PSK modulated signal. However, the MSJD framework has never been analyzed for an M-QAM primary signal.

In this work, the MSJD framework is analyzed for a primary M-QAM signal over a CSCG channel. Under the determined ranges, the framework appears to be convex. The simulated results clearly reflect that maximum secondary throughput is obtained when the primary signal is M-QAM modulated. The results are compared with the cases when the primary signal is binary phase-shift keyed (BPSK), CSCG, and modulated through a real modulation scheme.

II. Energy Detection in Individual Bands

To perform sensing on each individual subband independently, we decompose the received signal into L different waveforms, as illustrated in Fig. 1. We perform signal detection in each subchannel ℓ; when any of these subchannels are not being used by the secondary receiver, they can be used for opportunistic transmission [8]. Sensing each subchannel ℓ can be formulated as a binary hypothesis test as

$$R_\ell \sim \begin{cases} U_\ell & H_{0,\ell} \\ H_\ell S_\ell + U_\ell & H_{1,\ell} \end{cases} \qquad \ell = 1, 2, ..., L, \tag{1}$$

where $H_{0,\ell}$ denotes the situation in which the primary signal is absent from the ℓ-th subchannel and $H_{1,\ell}$ denotes the presence of the primary signal. It is assumed that each primary signal is M-QAM modulated and the channel is CSCG.

Energy detection is used to detect the presence or absence of primary signals in each subband in the allotted sensing slot τ. Consequently, the decision statistics of the ℓ-th subchannel using energy detection can be written as

$$T_\ell = \frac{1}{K} \sum_{k=1}^{K} | R_\ell(k) |^2 , \tag{2}$$

where K is the number of received samples in each subband. Figure 2 [2] depicts the frame structure for periodic spectrum sensing. Here, T is the frame length divided into one sensing slot τ and one data transmission slot $T-\tau$. The number of samples used for sensing each subchannel is $K = \tau f_s$, in which f_s is the system sampling frequency. Thus, the decision rule is given as follows:

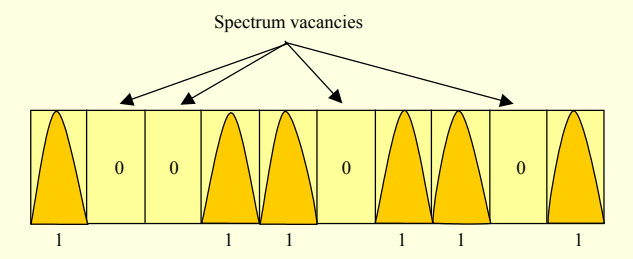

Fig. 1. Wideband channel divided into narrowband subchannels.

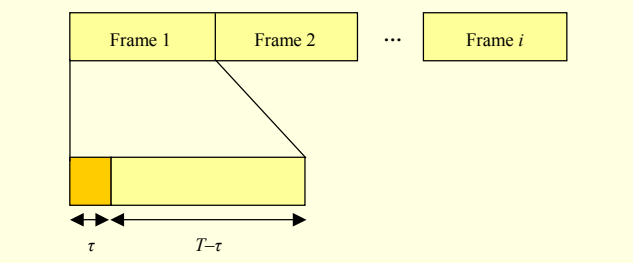

Fig. 2. Frame structure for periodic spectrum sensing.

$$T_\ell \underset{H_{1,\ell}}{\overset{H_{0,\ell}}{\gtrless}} \xi_\ell , \tag{3}$$

where ξ_ℓ is the decision threshold in subband ℓ. For a given threshold vector ξ and sensing time τ, the probability of false alarm and detection can be compactly represented as

$$\boldsymbol{P}_f(\xi, \tau) = \left[P_f^{(1)}(\xi_1, \tau), \ldots, P_f^{(L)}(\xi_L, \tau) \right]^T , \tag{4}$$

$$\boldsymbol{P}_d(\xi, \tau) = \left[P_d^{(1)}(\xi_1, \tau), \ldots, P_d^{(L)}(\xi_L, \tau) \right]^T , \tag{5}$$

$$\boldsymbol{P}_m(\xi, \tau) = \left[P_m^{(1)}(\xi_1, \tau), \ldots, P_m^{(L)} P(\xi_L, \tau) \right]^T . \tag{6}$$

The probability of missed detection is given by $\boldsymbol{P}_m(\xi, \tau) = \mathbf{1} - \boldsymbol{P}_d(\xi, \tau)$ and $\mathbf{1}$ denotes the vector made up of all ones. For successful detection, P_d should be as high as possible, while P_f should be kept as low as possible.

Definition 1. According to the central limit theorem, for a large number of samples, the probability distribution function (PDF) of $T_\ell(r)$, which is otherwise a chi-square distribution under both hypothesis $H_{0,\ell}$ and hypothesis $H_{1,\ell}$, can be approximated by a normal distribution. Let the PDF of $T_\ell(r)$ be defined as

$$T_\ell(r) \sim \begin{cases} \mathcal{N}\left(\mu_{0,\ell}, \sigma_{0,\ell}^2\right) & \text{under} \quad H_{0,\ell}, \\ \mathcal{N}\left(\mu_{1,\ell}, \sigma_{1,\ell}^2\right) & \text{under} \quad H_{1,\ell}, \end{cases}$$

where $\mu_{0,\ell}$ and $\mu_{1,\ell}$ represent the mean and variance for hypothesis $H_{0,\ell}$, $\sigma^2_{0,\ell}$ and $\sigma^2_{1,\ell}$ represent the mean and variance for hypothesis $H_{1,\ell}$, and $T_\ell(r)$ represents the test statistics of the received signal at each subband.

Lemma 1. When the primary signal is M-QAM modulated and the noise is CSCG, the decision rule is modified as

$$T_\ell(r) \sim \begin{cases} \mathcal{N}\left(\sigma_u^2, \sigma_u^4 / K\right) & \text{under } H_{0,\ell}, \\ \mathcal{N}\left(\sigma_u^2(\Upsilon_\ell + 1), \dfrac{1}{K}\sigma_u^4 \left(2\left(1 - \dfrac{1}{5}\dfrac{4M-1}{M-1}\right)\Upsilon_\ell^2 + 1 + 2\Upsilon_\ell\right)\right) & \text{under } H_{1,\ell}, \end{cases}$$

where $\Upsilon_\ell = \dfrac{\mathbb{E}(|S_\ell|^2)\,|H_\ell|^2}{\sigma_u^2}$ and E[·] denotes expectation.

Proof. For hypothesis $H_{1,\ell}$, mean $\mu_{1,\ell}$ is

$$\mu_{1,\ell} = \sigma_s^2 + \sigma_u^2 = \sigma_u^2\left(1 + \frac{\sigma_s^2}{\sigma_u^2}\right) = \sigma_u^2(1 + \Upsilon). \tag{7}$$

From [18], the variance $\sigma^2_{1,\ell}$ is

$$\sigma^2_{1,\ell} = \frac{1}{K}\left[\mathrm{E}|s(n)|^4 + \mathrm{E}|u(n)|^4 - \left(\sigma_s^2 - \sigma_u^2\right)^2\right]. \tag{8}$$

For M-QAM, $\mathrm{E}\{|s(n)|^4\}$ is given in [19] as $\mathrm{E}\{|s(n)|^4\} = 3 - \left(\dfrac{2}{5}\left(\dfrac{4M-1}{M-1}\right)\sigma_s^4\right)$. For the CSCG noise signal $\mathrm{E}\{|u(n)|^4\} = 2\sigma_u^4$, substituting the values $\mathrm{E}\{|s(n)|^4\}$ and $\mathrm{E}\{|u(n)|^4\}$ in (8), we get

$$\sigma^2_{1,\ell} = \frac{1}{K}\sigma_u^4\left(2\left(1 - \frac{1}{5}\frac{4M-1}{M-1}\right)\Upsilon_\ell^2 + 1 + 2\Upsilon_\ell\right). \tag{9}$$

For hypothesis $H_{0,\ell}$, since $\sigma_s^2 = 0$, mean $\mu_{1,\ell}$ and variance $\sigma^2_{0,\ell}$ from (6) and (8), respectively, are found to be

$$\mu_{0,\ell} = \sigma_u^2, \qquad \sigma^2_{0,\ell} = \sigma_u^4 / K. \qquad \square$$

Definition 2. The probability of false alarm for the ℓ-th subband is

$$P_f^{(\ell)}(\xi_\ell, \tau) = P_r(T_\ell > \xi_\ell \mid H_{0,\ell}) = \mathrm{Q}\left(\frac{\xi_\ell - \mu_{0,\ell}}{\sqrt{\sigma^2_{0,\ell}}}\right),$$

where $\mathrm{Q}(x) = \dfrac{1}{\sqrt{2\pi}}\displaystyle\int_x^\infty \exp\left(-\frac{t^2}{2}\right)dt$. Accordingly, P_f for CSCG noise is

$$P_f^{(\ell)}(\xi_\ell, \tau) = \mathrm{Q}\left(\left(\frac{\xi_\ell}{\sigma_u^2} - 1\right)\sqrt{\tau f_s}\right). \tag{10}$$

Definition 3. The probability of detection for the ℓ-th subband is defined as

$$P_d^{(\ell)}(\xi_\ell, \tau) = P_r(T_\ell > \xi_\ell \mid H_{1,\ell}) = \mathrm{Q}\left(\frac{\xi_\ell - \mu_{1,\ell}}{\sqrt{\sigma^2_{1,\ell}}}\right).$$

Accordingly, the probability of detection for the M-QAM signal and CSCG noise is

$$P_d^{(\ell)}(\xi_\ell, \tau) = \mathrm{Q}\left(\left(\frac{\xi_\ell}{\sigma_u^2} - \Upsilon_\ell - 1\right)\left(\sqrt{\frac{\tau f_s}{2\left(1 - \frac{1}{5}\frac{4M-1}{M-1}\right)\Upsilon_\ell^2 + 1 + 2\Upsilon_\ell}}\right)\right). \tag{11}$$

III. MSJD Framework for M-QAM Signal

In this section, the MSJD framework [4] for wideband spectrum sensing is presented (refer to Fig. 3). The objective of the problem is to optimize the performance of the secondary network. This is done by finding the optimal threshold vector $\boldsymbol{\xi} = [\xi_1, \xi_2, \xi_3, \ldots, \xi_L]^T$ and sensing time τ for the CR system to make efficient use of the unused spectrum without causing harm by interfering with the PUs.

1. Problem Statement

Let C_ℓ be the opportunistic throughput of the SU, at subchannel ℓ, when it operates in the absence of the PUs and $C = [C_1, C_2, \ldots, C_L]^T$. The available throughput can be defined as

$$R(\xi, \tau) = \left(\frac{T - \tau}{T}\right)C^T\left(\mathbf{1} - \boldsymbol{P}_f(\xi, \tau)\right), \tag{12}$$

where $1 - P_f^{(\ell)}$ is the vacancy in the spectrum detected by the

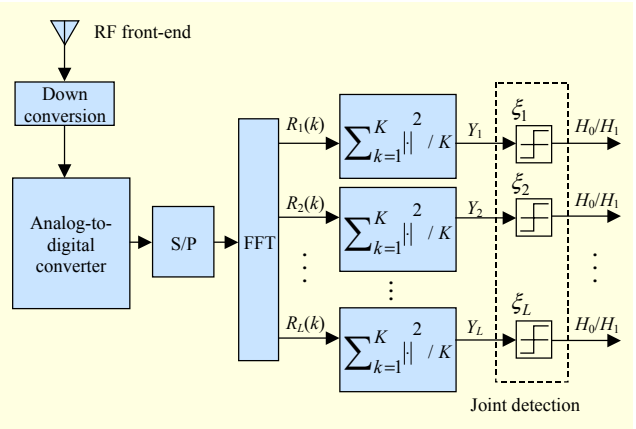

Fig. 3. Block diagram of MSJD framework [4].

SU and $(T–\tau)/T$ is the frame duration available for opportunistic transmission [9].

In a CR network, licensed users should experience limited interference. For a wideband primary communication system, the effect of interference induced by CR devices can be characterized by a relative priority factor for each PU transmitting over the corresponding subbands, that is, $\boldsymbol{\zeta} = [\zeta_1, \zeta_2, ..., \zeta_L]^T$, where ζ_ℓ is the cost of interfering with a PU in the ℓ-th subchannel [4]. Accordingly, the aggregate interference to the PU network can be defined as

$$Int_i(\xi, \tau) = \sum_{i \in S_i} \zeta_i P_m^{(i)}(\xi_i, \tau) \qquad i = 1, 2, ..., I. \tag{13}$$

For a single-user primary network, all subbands are used by one PU and I=1. Problem (P1), including four constraints, can thus be stated as

$$\begin{aligned} &\max_{(\xi,\tau)} \quad R(\xi, \tau), && \text{(P1)} \\ &\text{s.t.} \quad Int(\xi, \tau) \le \alpha\,, && \text{(C1)} \\ &\qquad \boldsymbol{P}_m(\xi, \tau) \preceq \beta, && \text{(C2)} \\ &\qquad \boldsymbol{P}_f(\xi, \tau) \preceq \gamma, && \text{(C3)} \\ &\qquad \tau \le \tau_{\max}\,, && \text{(C4)} \end{aligned}$$

where the maximum aggregate interference tolerated by the primary network is given by α. The missed detection and false alarm probabilities associated with each subband are $\beta = [\beta_1, \beta_2, ..., \beta_L]$ and $\gamma = [\gamma_1, \gamma_2, ..., \gamma_L]$. The maximum allowable sensing time is represented by $\tau_{\max}$.

2. Convex Optimization Problem for M-QAM Signal in MSJD Framework

In general, it is difficult to find the global solution for (P1) since both the objective function and the constraint function are nonconvex. However, this problem can be considered in the convex optimization category by exploiting the hidden convexity in the problem under some practical conditions. Due to false alarm and sensing-slot duration, there is an opportunistic throughput loss R_{loss}. Thus, the problem is reformulated to simplify analysis [4], [7] as

$$\min_{(\xi,\tau)} \quad R_{\text{loss}}(\xi, \tau), \tag{P2}$$

where $R_{\text{loss}}(\xi, \tau) = C^T \left[\boldsymbol{P}_f(\xi, \tau)\left(1 - \frac{\tau}{T}\right) + \mathbf{1}\frac{\tau}{T} \right]$. (14)

The constraints for (P2) are the same as the constraints for (P1).

To classify (P2) as a convex optimization problem, the objective function and constraints must be convex [18]. While (C1) consists of summation on the left-hand side of the inequality and a system design parameter for interference tolerance on the right-hand side, the constraint turns out to be convex. However, (C2) and (C3) are nonconvex, so we derive the associated probabilities and convexity ranges for the specific case (M-QAM primary signal) as follows.

3. Convexity of MSJD Framework for M-QAM Signal

The convexity range on P_f and P_d for the M-QAM modulated signal and CSCG noise case is as follows.

Lemma 2. The function $P_f^{(\ell)}(\xi_\ell, \tau)$ is convex in ξ_ℓ and τ if $P_f^{(\ell)}(\xi_\ell, \tau) \le \mathrm{Q}(1/\sqrt{3})$.

Proof. The Hessian of the above matrix can be calculated as

$$c_\ell \times \begin{bmatrix} \left(\frac{\xi_\ell}{\sigma_u^2} - 1\right)\frac{\tau^2 f_s}{\sigma_u^2} & \frac{\tau f_s}{2}\left(\frac{\xi_\ell}{\sigma_u^2} - 1\right)^2 - \frac{1}{2} \\ \frac{\tau f_s}{2}\left(\frac{\xi_\ell}{\sigma_u^2} - 1\right)^2 - \frac{1}{2} & \frac{\left(\frac{\xi_\ell}{\sigma_u^2} - 1\right)}{4\tau\sigma_u^{-2}} + \frac{\left(\frac{\xi_\ell}{\sigma_u^2} - 1\right)^3 f_s}{4\sigma_u^{-2}} \end{bmatrix}, \tag{15}$$

where $c_\ell = \frac{1}{\sigma_u^2}\sqrt{\frac{f_s}{2\tau\pi}} \exp\left(\frac{\tau f_s}{2}\left(\frac{\xi_\ell}{\sigma_u^2} - 1\right)^2 \right)$.

If $\left(\frac{\xi_\ell}{\sigma_u^2} - 1\right)\sqrt{\tau f_s} \ge \sqrt{\frac{1}{3}}$, then the determinant of (15), $Det(.) = c_\ell^2 \times \left(\frac{3}{4}\left(\frac{\xi_\ell}{\sigma_u^2} - 1\right)^2 \tau f_s - \frac{1}{4} \right)$, is nonnegative. Consequently, the matrix is positive semi-definite, implying that $P_f^{(\ell)}(\xi_\ell, \tau)$ is convex under the stated condition. □

Lemma 3. The function $P_m^{(\ell)}(\xi_\ell, \tau)$ is convex in ξ_ℓ and τ if $P_m^{(\ell)}(\xi_\ell, \tau) \le \mathrm{Q}(1/\sqrt{3})$.

Proof. The Hessian of the function can be calculated as

$$d_\ell \times \begin{bmatrix} \frac{\tau^2 f_s}{a_\ell \sigma_u^2}\left(\frac{\xi_\ell}{\sigma_u^2} - \Upsilon_\ell - 1\right) & \frac{\tau f_s}{2a_\ell}\left(\frac{\xi_\ell}{\sigma_u^2} - \Upsilon_\ell - 1\right)^2 - \frac{1}{2} \\ \frac{\tau f_s}{2a_\ell}\left(\frac{\xi_\ell}{\sigma_u^2} - \Upsilon_\ell - 1\right)^2 - \frac{1}{2} & \frac{\left(\frac{\xi_\ell}{\sigma_u^2} - \Upsilon_\ell - 1\right)}{4\tau\sigma_u^{-2}} + \frac{\left(\frac{\xi_\ell}{\sigma_u^2} - \Upsilon_\ell - 1\right)^3 \frac{f_s}{a_\ell}}{4\sigma_u^{-2}} \end{bmatrix}, \tag{16}$$

where $a_\ell = \left(2\left(1 - \frac{1}{5}\frac{4M-1}{M-1}\right)\Upsilon_\ell^2 + 1 + 2\Upsilon_\ell \right)$

and $d_\ell = \frac{1}{\sigma_u^2\sqrt{2\pi}}\sqrt{\frac{f_s}{\tau a_\ell}} \exp\left[-\left(\frac{\xi_\ell}{\sigma_u^2} - \Upsilon_\ell - 1\right)^2 \frac{\tau f_s}{2a_\ell} \right]$.

If $\sqrt{\frac{\tau f_s}{a_\ell}}\left(\frac{\xi_\ell}{\sigma_u^2}-\Upsilon_\ell-1\right)\geq\frac{1}{\sqrt{3}}$, then the determinant of (16), $Det(.)=d_\ell^2\left(\frac{\tau f_s}{a_\ell}\frac{3}{4}\left(\frac{\xi_\ell}{\sigma_u^2}-\Upsilon_\ell-1\right)^2-\frac{1}{4}\right)$, is nonnegative. Hence, P_d is concave for $P_d^{(\ell)}(\xi_\ell,\tau)\leq \mathrm{Q}(1/\sqrt{3})$, and P_m is convex under the condition since P_m=1–P_d. □

Lemma 4. The function $R_{\mathrm{loss}}(\xi,\tau)$ is convex in ξ_ℓ and τ if $P_f^{(\ell)}(\xi_\ell,\tau)\leq \mathrm{Q}(1/\sqrt{3})$ and $\tau/T\leq 0.5$.

Proof. The Hessian of the function can be calculated as

$$\begin{bmatrix} \left(1-\frac{\tau}{T}\right)\frac{\partial^2 P_f^{(\ell)}}{\partial \xi_\ell^{\,2}} & \left(1-\frac{\tau}{T}\right)\frac{\partial P_f^{(\ell)}}{\partial \xi_\ell \partial \tau}-\frac{1}{T}\frac{\partial P_f^{(\ell)}}{\partial \xi_\ell} \\ \left(1-\frac{\tau}{T}\right)\frac{\partial P_f^{(\ell)}}{\partial \xi_\ell \partial \tau}-\frac{1}{T}\frac{\partial P_f^{(\ell)}}{\partial \xi_\ell} & \left(1-\frac{\tau}{T}\right)\frac{\partial^2 P_f^{(\ell)}}{\partial \tau^2}-\frac{2}{T}\frac{\partial P_f^{(\ell)}}{\partial \tau} \end{bmatrix}. \quad (17)$$

It is positive definite for $P_f^{(\ell)}(\xi_\ell,\tau)\leq \mathrm{Q}(1/\sqrt{3})$ and $\tau/T\leq 0$ as proven in [8]. □

From [18], a nonnegative weighted sum of convex functions is a convex function. Hence, under Lemmas 2 through 4, both the objective function and the constraint function are convex if the following conditions are fulfilled:

$$0\leq \beta_\ell \leq \mathrm{Q}(1/\sqrt{3}),\ \ell=1,2,...,L, \quad (18a)$$

$$0\leq \gamma_\ell \leq \mathrm{Q}(1/\sqrt{3}),\ \ell=1,2,...,L, \quad (18b)$$

$$0\leq \tau_{\max}\leq 0.5T. \quad (18c)$$

IV. Simulation

The results are simulated by employing a two-stage algorithm, as proposed in [8], [9]. The steps involved are as follows:

Step 1. Select an initial sensing time τ.

Step 2. Select the tolerance.

Step 3. Run the first stage of the algorithm, in which the threshold vector is optimized (assuming a constant τ).

Step 4. Based on the threshold, the throughput loss R_{loss} obtained in Step 3 is $R_{\mathrm{loss}}^{\mathrm{previuos}}$.

Step 5. Calculate $\tilde{P}_m^\ell$.

Step 6. Run the 2nd stage of the algorithm, in which the optimum sensing slot duration τ is determined, assuming the threshold (obtained from Step 3).

Step 7. Based on the optimum sensing slot τ duration, the throughput loss R_{loss} obtained in Step 6 changes to $R_{\mathrm{loss}}^{\mathrm{next}}$.

Step 8. Repeat Step 3 through Step 7 of the algorithm iteratively based on updated values of ξ and τ, until the value of $\left|R_{\mathrm{loss}}^{\mathrm{previuos}}-R_{\mathrm{loss}}^{\mathrm{next}}\right|\prec$ tolerance and the solution are sufficiently accurate.

In the first stage of the algorithm, the threshold vector ξ is optimized (assuming a constant τ). Problem (P2) can accordingly be simplified into an equivalent form as

$$\min_{(\xi)} \quad R_{\mathrm{loss}}(\xi)=\sum_{\ell=1}^{L} C^T P_f^{(\ell)}(\xi_\ell), \quad (P3)$$

$$\text{s.t.} \quad Int_i(\xi)\leq \alpha_i, \quad (C5)$$

$$\xi_{\ell,\min}\leq \xi_\ell \leq \xi_{\ell,\max}, \quad (C6)$$

where $\xi_{\ell,\min}$ and $\xi_{\ell,\max}$ can be determined owing to the monotonically nonincreasing nature of the Q-function as

$$\xi_{\ell,\min}=\sigma_u^2\left(\sqrt{\frac{1}{\tau f_s}}\mathrm{Q}^{-1}(\gamma_\ell)+1\right)$$

and

$$\xi_{\ell,\max}=\sigma_u^2\left(\sqrt{\frac{a_\ell}{\tau f_s}}\mathrm{Q}^{-1}(1-\beta_\ell)+(\gamma_\ell+1)\right).$$

Although (C6) is linear, (P3) can be transformed into a convex optimization problem under the conditions that $0<\gamma_\ell\leq 1/2$ and $0<\beta_\ell\leq 1/2$.

To implement the second stage, we specifically exploit probabilities of missed detection $\boldsymbol{P}_m(\xi,\tau)$. There are four main parameters that are effective in determining probabilities of missed detection $\boldsymbol{P}_m(\xi,\tau)$: the achievable throughput C^T, the interference cost ζ_i, the channel signal-to-noise ratio (SNR) Υ_ℓ, and the sensing time τ. This information can be easily extracted from the objective and constraint functions in (P1).

We observe that the parameters C^T, ζ_i, and Υ_ℓ are channel-dependent values and sensing time τ is a channel-independent value. However, these channel dependency parameters are based on the simulation model, and, therefore, their values are fixed, causing the missed detection probabilities (that are computed in the first stage) to remain almost unchanged, even if the sensing time τ changes in the next iteration. Thus, we utilize this information to implement the second stage of the algorithm. Hence, in the second stage, we assume the probabilities of missed detection to be fixed values, $\tilde{P}_m^\ell$, obtained from the first stage. As a result, P_f is modified as

$$P_f^{(\ell)}=\mathrm{Q}\left(\sqrt{a_\ell}\mathrm{Q}^{-1}(1-\tilde{P}_m^\ell)+\Upsilon\sqrt{\tau f_s}\right). \quad (19)$$

Consequently, the optimization problem is reduced to

$$\min_{(\tau)} \quad R_{\mathrm{loss}}(\xi), \quad (P4)$$

$$\text{s.t.} \quad P_f^{(\ell)}(\tau)\leq \gamma, \quad (C7)$$

where

$$R_{\text{loss}}(\tau)=\sum_{\ell=1}^{L} C^{T}\left(\left(1-\frac{\tau}{T}\right)P_{f}^{(\ell)}(\tau)+\frac{\tau}{T}\right) \tag{20}$$

and $P_f^{(\ell)}$ is convex in the range $0 \le \gamma_\ell \le 0.5$. Since the optimization variable is only τ, the problem can be rewritten as

$$\min_{(\tau)} \quad R_{\text{loss}}(\xi) \ , \tag{P5}$$

$$\text{s.t.} \quad \tau \ge \arg\max\left\{\tau_{\min}^{(1)}, \tau_{\min}^{(2)}, \ldots, \tau_{\min}^{(\ell)}\right\}, \tag{C8}$$

where $\tau_{\min}^{(\ell)}$ is the minimum sensing time required at each subchannel, obtained by

$$\tau_{\min}^{(\ell)}=\frac{1}{\Upsilon^{2} f_s}\left[\mathrm{Q}^{-1}(\gamma)-\sqrt{a_\ell}\,\mathrm{Q}^{-1}(1-\tilde{P}_m^{(\ell)})\right]^{2}. \tag{21}$$

V. Numerical Results

In this section, computer simulation results are presented to evaluate the MSJD framework for the M-QAM signal using the energy detection sensing technique. Consider a 48-MHz wideband spectrum over which PU communication takes place. In this communication, orthogonal frequency division multiplexing modulation with eight subcarriers is adopted (that is, L=8). The received SNR Υ_ℓ, throughput rate (kbps) C^T, and the cost coefficient ζ_i are associated with each individual subchannel. Furthermore, the opportunistic spectrum utilization is at least 50% (that is, β=0.5), and the margin of opportunistic detection is at most 20% (that is, γ=0.2). Furthermore, the maximum time for which the SU network is unaware of the PU activity (that is, T) is selected such that Tf_s=3,000. One typical parameter set that is utilized for simulation is given in Table 1.

Figure 4 plots the maximum available throughput for CR transmission versus the aggregate interference in the primary network. It is evident that an M-QAM signal achieves a superior performance to that of a BPSK signal, a CSCG signal, and a real-valued Gaussian signal as a PU signal.

In Fig. 5, the available opportunistic throughput for CR transmission is plotted against the sensing time for M-QAM and the BPSK primary signal using the MSJD framework. We observe that the opportunistic throughput for CR transmission decreases as the sensing time increases. In other words, decreasing the sensing time increases the opportunistic throughput for CR transmission.

In Fig. 6, the first graph examines the effect of increasing the cost of interference with the PU on the threshold for the first subchannel, and the second graph examines the increasing cost of interference with the PU on the opportunistic throughput for the first subchannel. As the cost of interference increases, the corresponding threshold decreases to decrease the first subband

Table 1. Typical system parameter set used for the simulation.

ℓ	1	2	3	4	5	6	7	8
Υ_ℓ	0.38	1.37	0.32	0.24	0.35	0.27	0.39	0.38
C^T(kbps)	857	206	853	900	611	808	561	325
ζ_i	8.94	1.68	3.81	6.91	9.01	2.07	3.43	3.44

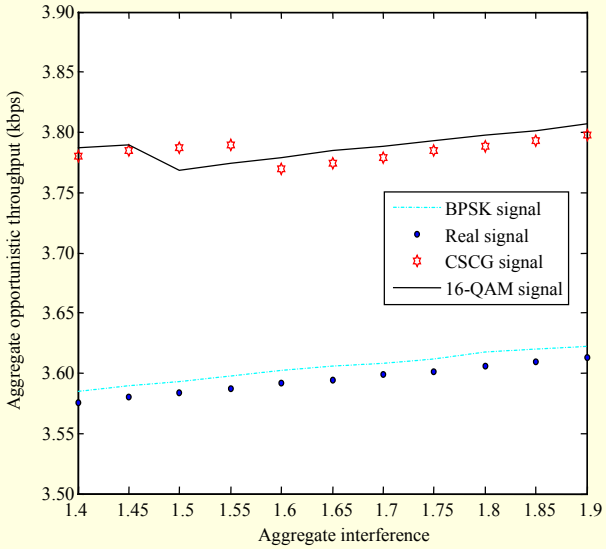

Fig. 4. Effect of variation of aggregate interference vs. aggregate opportunistic throughput in MSJD framework.

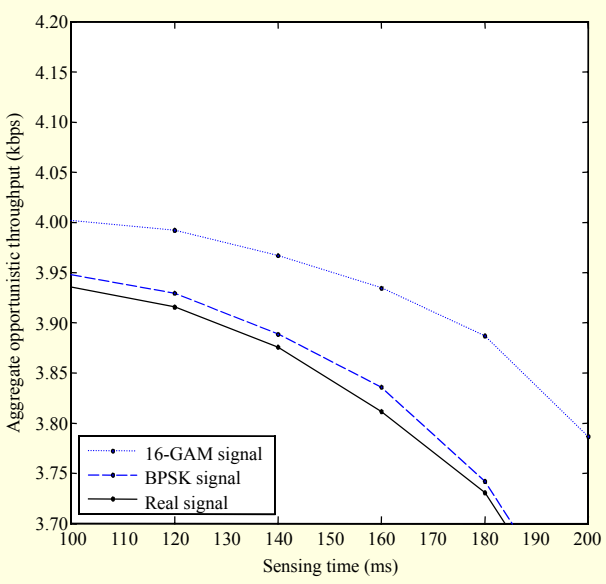

Fig. 5. Available opportunistic throughput vs. different primary signals in MSJD framework.

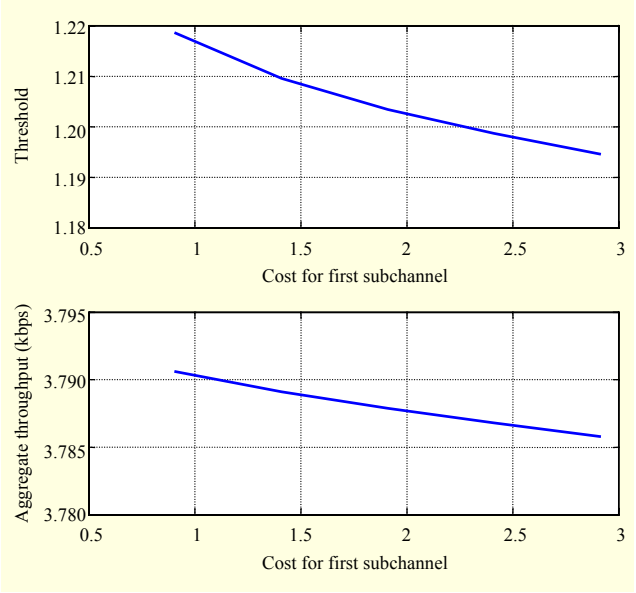

Fig. 6. Effect of variation of cost of interference vs. threshold.

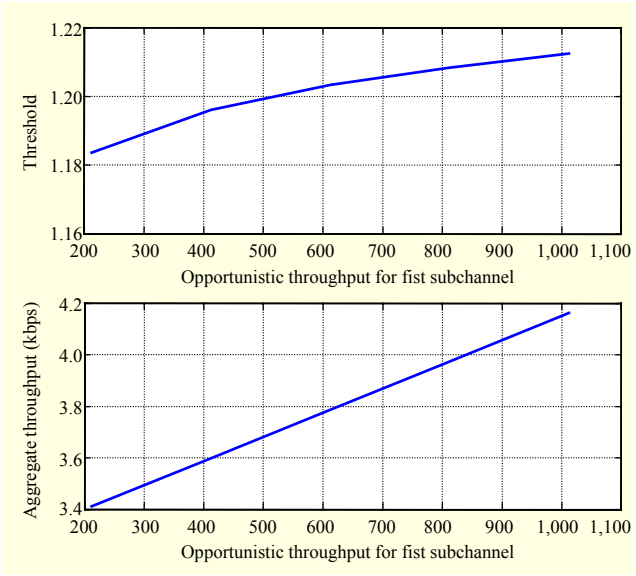

Fig. 7. Opportunistic throughput vs. threshold for first subchannel.

interference with the PU, causing the throughput to decrease.

In Fig. 7, the first graph is an analysis of the effect of increasing the opportunistic throughput for the first subchannel versus the threshold, and the second graph examines the effect of increasing the opportunistic throughput for the first subchannel versus aggregate throughput. An increase in opportunistic throughput C results in an increase of threshold ξ, such that the overall opportunistic throughput R increases.

VI. Conclusion

In this paper, to support periodic spectrum sensing, we considered media access control frame structure design. Mainly, we studied the problem of designing both the sensing slot duration and threshold to maximize the achievable throughput for SUs under the constraints that the PUs are protected from interference from the SUs. An optimal framework for wideband spectrum sensing, referred to as MSJD, was analyzed for a M-QAM primary signal and a CSCG channel to maximize the achievable opportunistic throughput of the SU while keeping the interference with the PU network limited. The problem that was formulated seemed to be nonconvex, but, by applying practical constraints on it, proved to be a convex optimization problem for M-QAM primary signals and the CSCG channel noise condition. Results were compared with BPSK and real-valued Gaussian primary signals and CSCG or real-valued Gaussian noise.

References

[1] J. Mitola and G.Q. Maguire, "Cognitive Radio: Making Software Radios More Personal," *IEEE Personal Commun.*, vol. 6, no. 14, Aug. 1999, pp. 13-18.

[2] I.F. Akyildiz et al., "NeXt Generation/Dynamic Spectrum Access/Cognitive Radio Wireless Networks: A Survey," *Comput. Netw. (Elsevier)*, vol. 50, no. 13, Sept. 2006, pp. 2127-2159.

[3] S. Haykin, "Cognitive Radio: Brain-Empowered Wireless Communications," *IEEE J. Sel. Areas Commun.*, vol. 23, no. 2, Feb. 2005, pp. 201-220.

[4] Z. Quan et al., "Optimal Multiband Joint Detection for Spectrum Sensing in Cognitive Radio Networks," *IEEE Trans. Signal Process.*, vol. 57, no. 3, Mar. 2009, pp. 1128-1140.

[5] Z. Quan et al., "Spatial-Spectral Joint Detection for Wideband Spectrum Sensing in Cognitive Radio Networks," *Proc. IEEE Int. Conf. Acoustic, Speech, Signal Process.*, Apr. 2008, pp. 2793-2796.

[6] Z. Quan et al., "Collaborative Wideband Sensing for Cognitive Radios," *IEEE Signal Process. Mag.*, vol. 25, no. 6, Nov. 2008, pp. 60-73.

[7] P.P. Hoseini and N.C. Beaulieu, "Optimal Wideband Spectrum Sensing Framework for Cognitive Radio Systems," *IEEE Trans. Signal Process.*, vol. 59, no. 3, Mar. 2011, pp. 1170-1182.

[8] P.P. Hoseini and N.C. Beaulieu, "An Optimal Algorithm for Wideband Spectrum Sensing in Cognitive Radio Systems," *Proc. IEEE Int. Conf. Commun.*, May 2010.

[9] S.Z. Farooq and A. Ghafoor, "Multiband Joint Detection Framework for Complex Gaussian Signals in Cognitive Radios," *Proc. IEEE 22nd Int. Symp. Personal, Indoor Mobile Radio Commun. (PIMRC)*, Sept. 2011, pp. 493-497.

[10] S. Xie et al., "A Parallel Cooperative Spectrum Sensing in Cognitive Radio Networks" *IEEE Trans. Veh. Technol.*, vol. 59, no. 8, 2010, pp. 4079-4092.

[11] R.L. Valcarce and G.V. Vilar, "Wideband Spectrum Sensing in Cognitive Radio: Joint Estimation of Noise Variance and Multiple Signal Levels," *IEEE Workshop Signal Process. Adv. Wireless Commun.*, 2009, pp. 96-100.

[12] A. Sahai and D. Cabric, "A Tutorial on Spectrum Sensing: Fundamental Limits and Practical Challenges," *Proc. IEEE Symp. New Frontiers Dynamic Spectrum Access Netw.*, Baltimore, MD, USA, Nov. 2005.

[13] Z. Tian, "Compressed Wideband Sensing in Cooperative Cognitive Radio Networks," *Proc. IEEE GLOBECOM*, 2008, pp. 1-5.

[14] A. Taherpour, S. Gazor, and M.N. Kenari, "Invariant Wideband Spectrum Sensing under Unknown Variances," *IEEE Trans. Wireless Commun.*, 2009, vol. 8, no. 5, pp. 2182-2186.

[15] K. Hossain and B. Champagne, "Wideband Spectrum Sensing for Cognitive Radios with Correlated Subband Occupancy," *IEEE Signal Process. Lett.*, vol. 18, no. 1, Jan. 2011, pp. 35-38.

[16] I.F. Akyildiz, B.F Lo, and R. Balakrishnan, "Cooperative Spectrum Sensing in Cognitive Radio Networks: A Survey," *ELSEVIER Physical Commun.*, vol. 4, 2011, pp. 40-62.

[17] A. Latif, *Hybrid QAM - FSK (HQFM) OFDM Transceiver with Low PAPR*, doctoral dissertation, Faculty of Electronic Engineering, Ghulam Ishaq Khan Institute of Engineering Sciences and Technology, Pakistan, 2009.

[18] S. Boyd and L. Vandenberghe, *Convex Optimization*, Cambridge, UK: Cambridge University Press, 2003.

[19] H. Mathis, "On the Kurtosis of Digitally Modulated Signals with Timing Offsets," *3rd IEEE Signal Process. Workshop Signal Process. Adv. Wireless Commun*., Taoyuan, Taiwan, Mar. 2001, pp. 86-89.

Sana Tariq received her BS in electronic engineering from Islamia University of Bahawalpur (IUB), Bahawalpur, Punjab, Pakistan, in 2009 and MS in electrical engineering from the National University of Sciences and Technology (NUST), Islamabad, Pakistan, in 2012. Her research interests include cognitive radio networks and wireless communications.

Abdul Ghafoor received his BS in electrical engineering from the University of Engineering and Technology, Lahore, Pakistan, in 1994, his MS in electrical engineering from the National University of Sciences and Technology (NUST), Islamabad, Pakistan, in 2003, and his PhD from the University of Western Australia (UWA), Perth, Western Australia, Australia, in 2007. His research topics include model/controller order reduction, image processing/matching, through-wall imaging, and cognitive radio. Since 2008, he has been with NUST, where he is currently an associate professor.

Salma Zainab Farooq received her BS and MS in electrical engineering from the University of Engineering and Technology, Taxila, Punjab, Pakistan, and the National University of Sciences and Technology (NUST), Islamabad, Pakistan, respectively. She has been involved in research on signal processing for communications for 10 years. Having worked at Communication Enabling Technologies porting VOIP algorithms over custom designed media engines, she joined the Institute of Space Technology (IST), Islamabad, Pakistan, in 2004, where she is currently a lecturer in the Electrical Engineering Department and teaches communication systems and digital signal processing to undergraduate students.